

Finite Element Simulation of a Surface Acoustic Wave driven Linear Motor using COMSOL Multiphysics

Basudeba Behera^a, Harshal B. Nemade^a, Shyam Trivedi^a

^aIndian Institute of Technology Guwahati, Guwahati, Assam, 781039, India

basudeba@iitg.ernet.in

Abstract: The paper presents finite element simulation of a surface acoustic wave (SAW) linear motor. The function of SAW linear motor depends on the principle of friction drive provided by SAW propagating on a piezoelectric substrate. The SAW motor comprises of a slider driven by Rayleigh wave generated on a piezoelectric stator using an interdigital transducer (IDT) fabricated on surface of the stator. In the simulation, a lithium niobate piezoelectric substrate is used as the stator on which aluminum IDTs are fabricated at the two side ends and a cuboid slider with preload is placed in the path of SAW propagation. The characteristics of displacement, velocity, and forces acting on the slider for continuous wave excitation are studied. The slider in the SAW motor can move in both forward and reverse directions and the motor attains a velocity of 0.3 m/s with the continuous wave excitation.

Keywords: *Lithium niobate (LN), Rayleigh wave, SAW motor, USM*

1. Introduction

The piezoelectric materials have facilitated miniaturization of motors, and several mechanisms to construct ultrasonic motors have been reported [1]. The advent of surface acoustic wave (SAW) motors led to improved resolution and high-power-density operation [2]. Persistent development in SAW motors resulted in light-weight devices, very high speed, and feasibility of sub-nanometer stepping resolution [3]. The motor consists of a 128° rotated Y cut X propagating lithium niobate (LiNbO₃) or (LN) substrate used as stator where aluminum (Al) electrodes are fabricated in the shape of comb structure called as interdigital transducers (IDTs) at both side ends as shown in Figure 1 [4]. A cuboid slider having cylindrical projections is tightly placed on the active region of the delay line of the stator. Rayleigh wave is generated and propagated on the surface of the stator when an RF power is applied to the IDTs. The components on the surface of the stator makes elliptical motion that drives the slider in the direction opposite to SAW propagation.

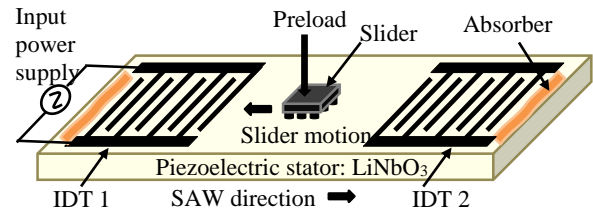


Figure 1: Schematic of piezoelectric SAW motor.

2. Design of stator

In order to determine the required frequency for wave excitations on the surface of stator to generate the Rayleigh wave, the Eigen frequency analysis is carried out in 3-D environment of COMSOL Multiphysics. The converse piezoelectricity property of the LN piezoelectric stator is used for operation of this device. The property states that the strain produced in the substrate is proportional to the magnitude of the applied electric signal [5].

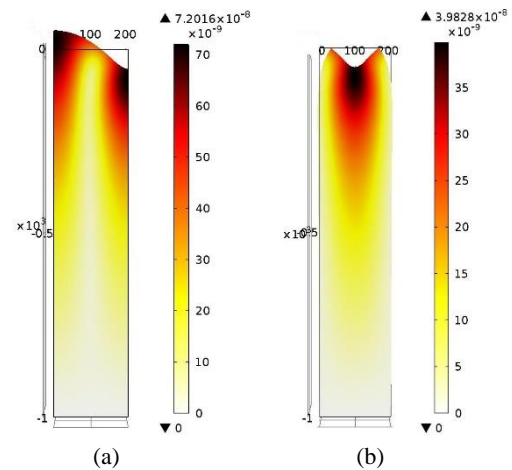


Figure 2: Displacement profile showing (a) resonance and (b) anti-resonance in a resonator

IDT of 400 μm wavelength (λ) is made on the surface of LN substrate as stator. A section of $\lambda/2$ length is simulated with antiperiodic boundary condition for side walls.

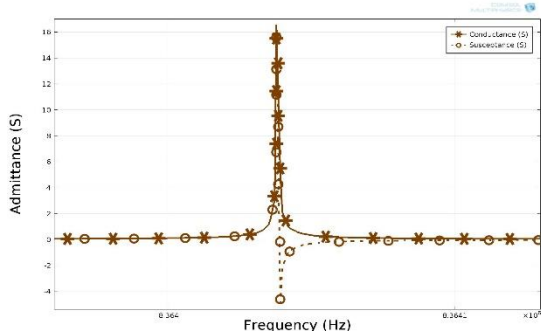


Figure 3: Admittance plot of the resonator.

Admittance plot for the above described structure given in Figure 3 shows the resonance frequency 8.37 MHz which is used for input power supply in subsequent simulations.

3. FE simulation of SAW motor

The FE simulation of the SAW motor is performed in COMSOL Multiphysics using the coupling of piezoelectric and solid mechanics physics.

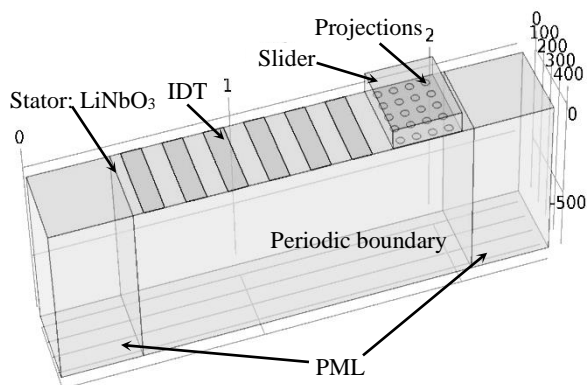


Figure 4: Schematic of SAW motor model.

A silicon cuboid slider having projections on its surface is tightly placed over an LN stator with the help of preload to maintain appropriate contact pressure between the slider and the stator as shown in Figure 4.

3.1 Modeling SAW motor

This section deals with constructing the SAW motor geometry and setting up multiphysics.

3.1.1. The geometry of SAW motor

The 3D plane geometry of a delay line consists of IDT electrodes of aperture 400 μm (1λ), width 100 μm ($\frac{1}{4} \lambda$) and thickness 0.2 μm on a LN substrate of width 400 μm (1λ), length 2150 μm and height 800 μm (2λ). The device is terminated with

perfectly matched layer (PML) of width 400 μm (1λ) as shown in Figure 4 to avoid reflections at the edges.

A silicon slider of size 400 μm x 400 μm x 100 μm is placed in the active region of the delay line. To avoid the problem of sticky surfaces, cylindrical projections of diameter 20 μm and center to center space of 40 μm are made on the surface of the slider in contact with the stator.

3.1.2. Assigning materials

In the SAW linear motor the stator is assigned with 128° rotated Y-cut X-propagating LiNbO₃ piezoelectric material. The elastic coefficients, Young's modulus, Poisson's ratio and density values are specified [6]. The comb shaped metal electrodes are assigned with aluminum (Al) material due to its light weight and high conductive property. The cubical slider along with the cylindrical projections is assigned with silicon (Si) material as fabricating projections in Si is easy [7].

3.1.3. Multiphysics settings

In subdomain settings, the stator is assigned as piezoelectric element. The comb shaped electrodes and slider are declared as linear element. The comb shaped IDTs are assigned with electric elements to apply input power.

Boundary setting plays a vital role in simulating the device. The boundary settings in the simulation are as follows. The slider and the stator form a contact pair with the stator as the master and the slider as the slave. The side boundary of the slider is kept free. The bottom of the stator is fixed while the ends are terminated with PML to avoid reflections. Periodic boundary condition is applied along the aperture. The parameters used for simulation are given in Table 1.

Table 1: Parameters for FE simulation

Parameters	Value	Units
Young's modulus of slider	169	GPa
Young's modulus of stator	173	GPa
Poisson's ratio of slider	0.3	-
Poisson's ratio of stator	0.345	-
Frequency	8.37	MHz
Preload	1.66	mN
Static coefficient of friction	0.45	-
Dynamic coefficient of friction	0.15	-
Radius of the projections	20	μm
Mass of the slider	0.4	mg
Input voltage	100	V

3.1.4. Mesh settings

The entire SAW motor is divided into small parts for meshing. Triangular mesh is applied to the boundaries of the device, then whole domain is meshed under swept meshing.

3.2. Results

When the Rayleigh wave propagates on the surface of the stator in a ultrasonic motor, the displacement of surface components in normal (u_z) and translational (u_x) directions can be found as [8],

$$u_z = a_z \sin(\omega t) \quad (1)$$

$$u_x = -a_x \cos(\omega t) \quad (2)$$

where, a_z is the amplitude of wave in normal direction, a_x is the amplitude of wave in translational direction, and ω is the angular frequency.

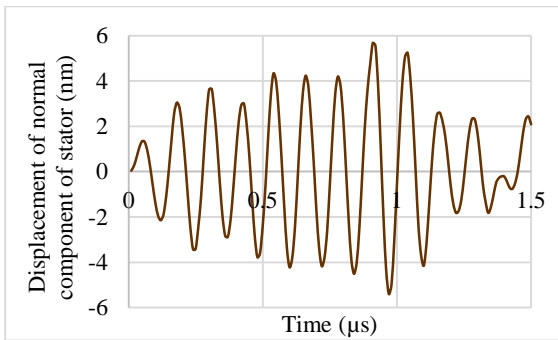


Figure 5: Displacement of normal component of stator.

With the application of 100 V, 8.37 MHz sine wave input, the normal displacement and translational displacement at a point on the stator surface are shown in Figure 5 and Figure 6, respectively.

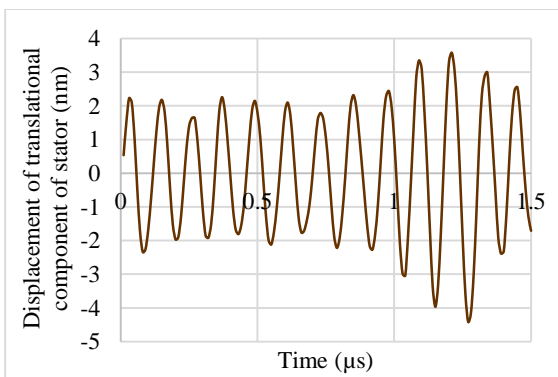


Figure 6: Displacement of translational component of stator.

The slider makes tight contact with the stator with the application of preload from the top. The Rayleigh wave makes a frictional contact at the bottom surface of the slider and displaces the slider as shown in Figure 7.

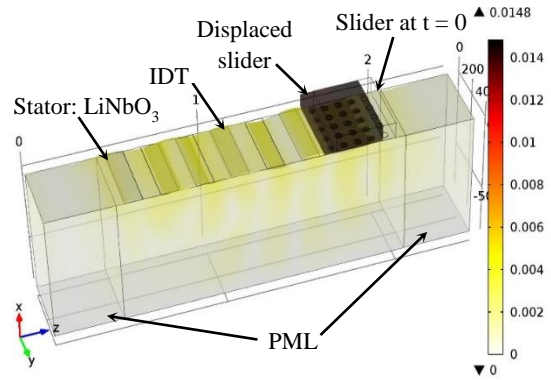


Figure 7: Displacement profile showing surface vibrations and slider movement after 1.5 μ s.

At the crest of the wave the slider sticks with the wave and frictional force acting on the slider moves it in the direction of motion of the stator surface. At the trough of the wave the slider makes another contact with the wave but the force transmitted to the slider is not significant. The rest of the time the slider is not pushed as it is not in contact with the wave and the state is called as slip condition [9].

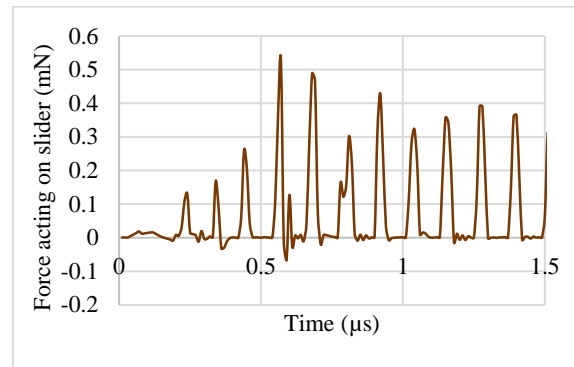


Figure 8: Translational force acting on the slider.

The translational force is acting on the slider through contact between slider and stator due to propagation of SAW is as shown in Figure 8. This force makes the slider to move in desired direction and path. The motion of the slider can be resolved into normal and translational components. The oscillation of the slider in normal direction diminishes with time as shown in Figure 9.

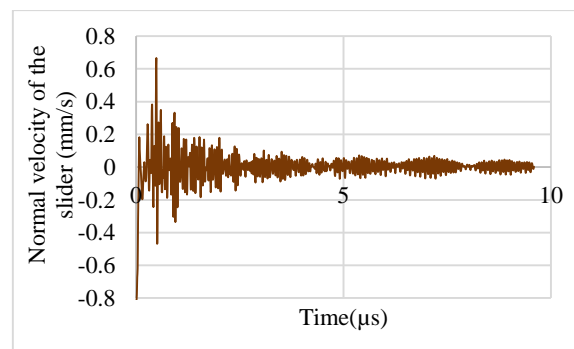


Figure 9: Motion of the slider in normal direction.

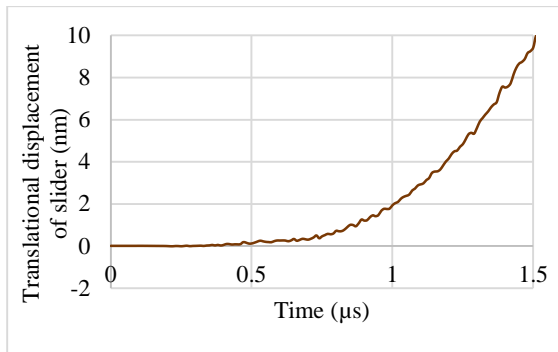


Figure 10: Translational motion of the slider.

Continuous wave excitation results in the translational displacement of the slider of 10 nm during initial 1.5 μs as shown in Figure 10.

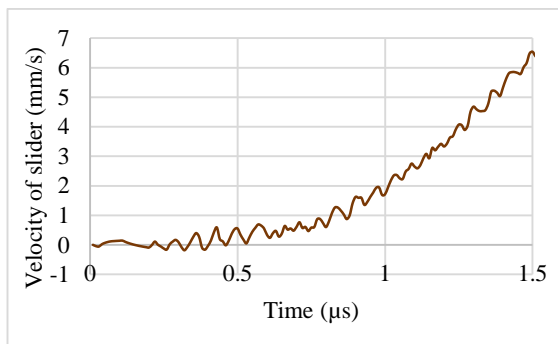


Figure 11: Velocity of the slider

The plot for the velocity of the slider shown in Figure 11 indicates step change in motion for every cycle of the excitation. The velocity stabilizes to 0.3 m/s after the application of continuous wave excitation for about 1 s.

When the IDTs are placed on both sides of the stator, the motor can be operated to move in both forward and reverse directions. When IDT 1 in Figure 1 is activated, the Rayleigh wave propagates on the stator towards IDT2 and the slider will move towards IDT1. If IDT1 is deactivated and IDT2 is activated, the wave will start propagating towards IDT1 and the slider will move towards IDT2. Thus the position of the slider on the surface of the stator can be controlled by actuating appropriate IDTs.

5. Conclusions

A SAW motor is simulated in COMSOL Multiphysics. The translational force acting on the slider due to propagation of Rayleigh wave under the slider is observed. The displacement of the slider in normal and translational directions are observed.

References

- [1] C. Zhao, *Ultrasonic Motors Technologies and Applications*, First Edit. Nanjing, China: Springer Publication, 2011.
- [2] M. K. Kurosawa, "Ultrasonic linear motor using traveling surface acoustic wave," in *Proceedings of IEEE Ultrasonics Symposium*, 2009, pp. 1096–1105.
- [3] T. Shigematsu, M. K. Kurosawa, and K. Asai, "Sub-nanometer stepping drive of surface acoustic wave motor," in *Proceedings of IEEE Conference on Nanotechnology*, 2003, vol. 2, pp. 299–302.
- [4] A. V. Mamishev, K. Sundara-Rajan, F. Yang, Y. Du, and M. Zahn, "Interdigital Sensors and Transducers," in *Proceedings of the IEEE*, 2004, vol. 92, no. 5, pp. 808–845.
- [5] A. A. Vives, *Piezoelectric Transducers and Applications*, Second Edi. Spain: Springer-Verlag Berlin Heidelberg, 2008.
- [6] K. K. Wong, *Propeties of lithium niobate*. London: INSPEC, The Institution of Electrical Engineers, 2002.
- [7] V. Lindroos, M. Tilli, A. Lehto, and T. Motooka, *Handbook of silicon based MEMS materials and Technologies*. Burlington: William Andrew, 2010.
- [8] T. Shigematsu and M. K. Kurosawa, "Friction Drive of an SAW Motor. Part III : Modeling," *IEEE Trans. Ultrason. Ferroelectr. Freq. Control*, vol. 55, no. 10, pp. 2266–2276, 2008.
- [9] T. Morita, M. K. Kurosawa, and T. Higuchi, "Simulation of Surface Acoustic Wave Motor with Spherical Slider," *IEEE Trans. Ultrason. Ferroelectr. Freq. Control*, vol. 46, no. 4, pp. 929–934, 1999.